

Electron Beam Weldability of Pure Magnesium and AZ31 Magnesium Alloy *

Toshikatsu Asahina and Hiroshi Tokisue

College of Industrial Technology, Nihon University, Narashino 275-8575, Japan

Pure magnesium and AZ31 magnesium alloy plates 4 mm in thickness were butt welded without addition of filler wire using a high voltage electron beam welding machine. Mechanical properties and microstructures of the welded joints were investigated. Regardless of the materials, the welded joints were almost free from welding defects and showed good bead appearance under appropriate welding conditions. The arcing phenomena tend to appear at low welding speed. Optimum beam current and welding speed were smaller than those for electron beam welded joints of aluminum alloys. Hardness in the fusion zone of the joints are nearly equal to those of the base metals. Microstructure on the fusion zone of pure magnesium joints was remarkably coarse, although the weld interface could not unambiguously detected. The fine crystal grains observed on the fusion zone of AZ31 alloy joints. Regardless of the welding conditions, both tensile strength and ductility of the joints show same value to those of the base metals, but the elongation of the joints are inferior to those of the base metals. From the tension test and impact test, pure magnesium joints fractured at the center of the fusion zone, but in case of AZ31 alloy joints, crack occurred at weld interface and it propagated through the fusion zone.

(Received June 25, 2001; Accepted September 3, 2001)

Keywords: pure magnesium, AZ31 magnesium alloy, electron beam welding, microstructure, mechanical properties

1. Introduction

Although electron beam welding is a kind of fusion welding, it is less affected by oxidation or gases than TIG welding since it melts and solidifies the base metal in a vacuum. In addition, the base metal is rapidly heated directly under a beam and evaporated locally forming beam holes.

Molten metal around them flows into the holes and forms a bead. In general, electron beam welding is considered to be applicable for the welding of aluminum alloys which can be easily welded with inert gas arc welding.¹⁾ On the other hand, in the welding of magnesium alloys, welding is apt to be disrupted by arcing phenomenon since their vapor pressure is high. Furthermore, beam holes which are bigger than other metals are apt to be produced causing the occurrence of blowholes in the fusion zone since melting point is low, and burn-through easily occurs due to the low surface tension of the molten metal, it is thought. Authors have already reported on the mechanical properties of electron beam welded joints of AZ80 magnesium alloy.²⁾ As a result, it has been clarified that joints with high joint efficiency can be obtained easily by the selection of optimum welding conditions and electron beam welding is also applicable for magnesium alloys.

In this research, electron beam butt welding of pure magnesium and AZ31 magnesium alloy, which are in actual use as structural materials, was carried out at various welding speeds. The structures and mechanical properties of the joints obtained by the tests were studied and comparative examinations of the weldability of the two test materials were conducted.

2. Materials and Experimental Procedure

Chemical compositions and mechanical properties of pure

magnesium and AZ31 magnesium alloy extruded material (hereinafter called pure Mg and AZ31 alloy, respectively) used as test materials are shown in Table 1. They were machined by cutting down to 55 mm width × 50 mm length × 4 mm thickness and degreased their welding surfaces with a wire brush just before welding.

A high voltage electron beam (hereinafter called EB) welding machine of 6 kW maximum output was used for welding and the initial vacuum of welding chamber was set at 3×10^{-3} Pa. Welding conditions are shown in Table 2. In regard to beam current and active beam parameters (ab value), conditions which assure full penetration to the base metals but will not cause burn-through were selected referring to preliminary experiments. The range of EB welding conditions which was selected for magnesium alloys was narrower than that for aluminum alloys.³⁾ This is because the surface tension of molten pure Mg, 559 mN/m, is only about a half of that of pure aluminum, 914 mN/m, and is liable to cause burn-through.

The specimens were clamped with welding jigs with a 40 N·m torque and secured in place in order to prevent irregularity due to deformation during welding. Copper backing plates were used for preventing burn-through. The specimens were welded at right angle to the extruding direction of the test materials and square butt welding without root gap was carried out without using any filler wire.

The hardness distribution of the joints after welding were measured at the depth of about 1.2 mm from the surface of the center of the bead and at intervals of 0.2 mm from the center of the bead toward both the base metals, using a micro Vickers hardness tester (load: 0.49 N).

The excess weld metal of surface and penetration beads were cut down and JIS #7 tensile test specimens with the center of the fusion zone as the gauge center and JIS #4 sub-size impact test specimens (width: 2.5 mm) with a V-notch at the center of the fusion zone were prepared. Bending test was carried out with the roller tip of 14 mm diameter and setting the center of fusion zone to that of the test specimens.

*This Paper was Originally Published in the Journal of Japan Institute of Light Metals 50 (2000) 512-517.

Table 1 Chemical compositions and mechanical properties of base metals.

Materials	Chemical compositions (mass%)								Tensile strength (MPa)	Elongation (%)	Impact value (kJ/m ²)	Hardness (HV0.5)
	Al	Zn	Mn	Fe	Si	Cu	Ni	Mg				
Pure Mg	0.004	0.005	0.003	0.003	0.003	0.001	0.001	bal.	144	9	41	38
AZ31 magnesium alloy	3.00	0.90	0.31	—	0.02	—	—	bal.	247	24	55	55

Table 2 Electron beam welding conditions for pure magnesium and AZ31 magnesium alloy.

Accelerating voltage	(kV)	150
Beam current	(mA)	5
Active beam parameter		1.3
Welding speed	(mm/s)	3.75, 4.17, 4.58, 5.00, 5.83, 6.67

3. Experimental Results and Discussion

3.1 Observation of bead appearance and macrostructure and microstructure

Effect of welding speed on bead appearances is shown in Fig. 1. No arcing phenomenon was observed at any welding conditions. Both surface and penetration beads showed comparatively smooth and uniform bead widths, regardless of the welding speed. Neither difference in bead appearances due to welding speed nor change in bead width from the beginning of the weld to the end is observed. Surface bead width

at the welding speed of 5.00 mm/s is the narrowest at about 0.8 mm. The surface beads are slightly concave since no filler wire was used but burn-through at the beam end was less compared with TIG welded joints.⁴⁾ In addition, burn-through of penetration beads was also less, but a small amount of spatter was generated.

Examples of macrostructure in the cross-section and surface of welds are shown in Fig. 2. They show well-type penetration profile regardless of the test materials and penetration profile extended to the reverse surface. As the result of inspection of five cross-sections of five specimens of each welding condition, neither cracks nor blowholes were observed. Bead width decreased along with the increase of welding speed. A tendency was observed that the penetration bead width of the pure Mg becomes slightly wider in comparison with that of the AZ31 alloy.

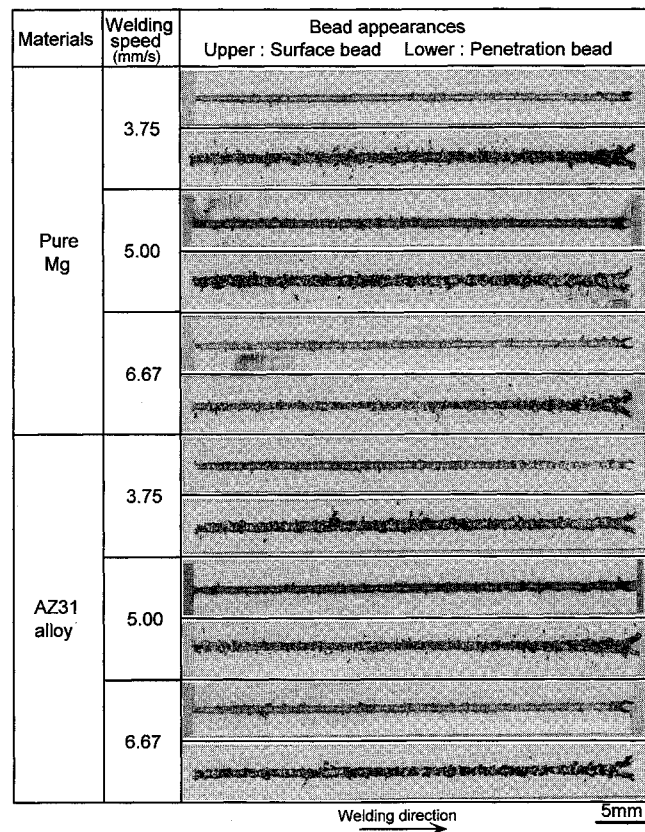


Fig. 1 Effect of welding speed on bead appearances of electron beam welded pure magnesium and AZ31 magnesium alloy joints.

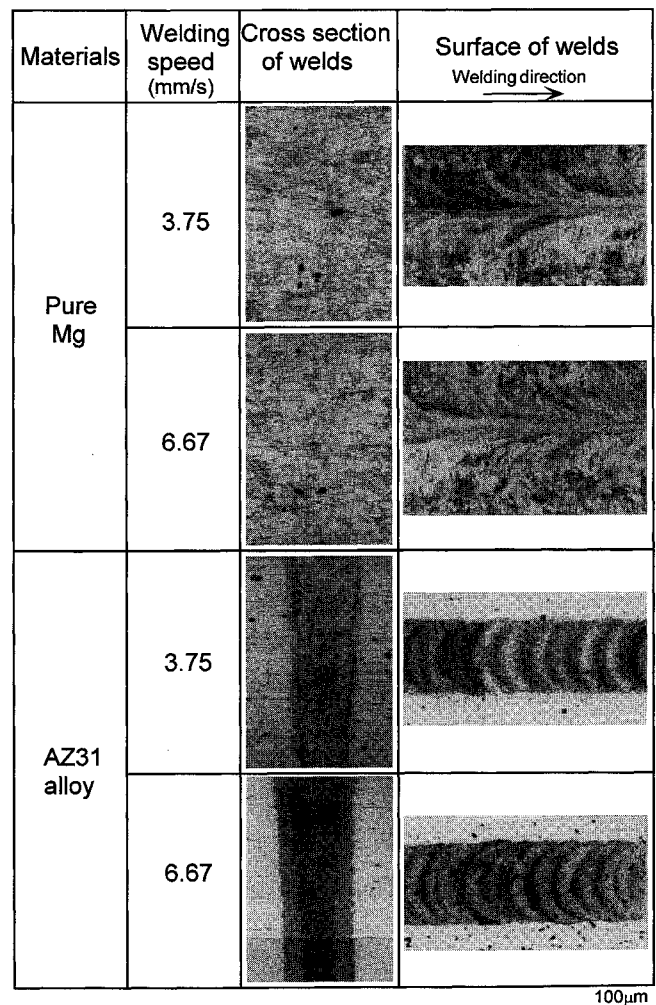


Fig. 2 Macrostructures of electron beam welded joints.

In the cross-sectional structure of the pure Mg, interfaces between heat affected zones and fusion zones are obscure and grain boundaries are also not clear. This has also been observed in friction welded pure Mg joints.⁵⁾ Ripple lines are not observed on the surface structure of the joint and the width in the center of the fusion zone slightly narrows as welding speed increases. Columnar crystals grow from the weld interface toward welding direction and their length tends to decrease slightly as welding speed increases. Furthermore, stray crystals parallel to welding direction in the center of the fusion zone are observed.

In regard to the cross-sectional structure of the AZ31 alloy, the width of the center of the fusion zone became narrower as welding speed increased and stratified structures were observed within the fusion zone. Close observation of this structure clarifies the crystal grains in the darkly corroded area are slightly finer than those in the white area, similar to ripple lines, and it is surmised that there were differences in the cooling speed of molten metal. The cross-sectional area of molten metal is 3.2 mm^2 and is considerably smaller than that of TIG welding of 24 mm^2 . This phenomenon indicates that molten metal was extremely rapidly heated and cooled and, at the same time, the metal discontinuously solidified due to the agitation of molten metal in the molten pool, which is unique to EB welding, and quenching action, it is thought. In the case of AZ31 alloy, ripple lines are clearly observed in the surface structure and their intervals are tend to become narrower as welding speed increases.

Figure 3 shows the microstructure of the cross-section of the joints at the welding speed of 5.00 mm/s . The crystal grains in the pure Mg fusion zone as shown in (a) are coarser than those of the base metal and twins are observed in the crystal grains. The weld interface is not observed clearly, columnar crystals grew from the heat affected zone toward the fusion zone and equi-axed grains are observed at the center of the fusion zone. This phenomenon is observed regardless of welding speed. Columnar crystals in the fusion zone grew due to the fusion of a part of the coarsened grains of the crystal grains in the heat affected zone with those of the fusion zone. The width of crystal grains in the fusion zone adjacent to weld interface and that of columnar crystals were the same. In the weld interface so-called epitaxially grown columnar crystals, that is a part of the base metal is melted by welding heat and molten metal grows on the remaining crystal grains at the time of solidification, were observed. It is presumed, therefore, that in the case of the pure Mg, of which crystal grains of the base metal are apt to coarsen during welding, columnar crystals in the fusion zone became big.

The structure of the AZ31 alloy fusion zone is equi-axed grains as shown in (b) and is extremely finer than that of the base metal. This structure is a typical quenched cast structure. The crystal grains observed in the darkly corroded area in the fusion zone are finer than those in the other areas. The interface between the heat affected zone and the fusion zone can be clearly observed and there is a clear difference in grain sizes. Furthermore, on close observation of the microstruc-

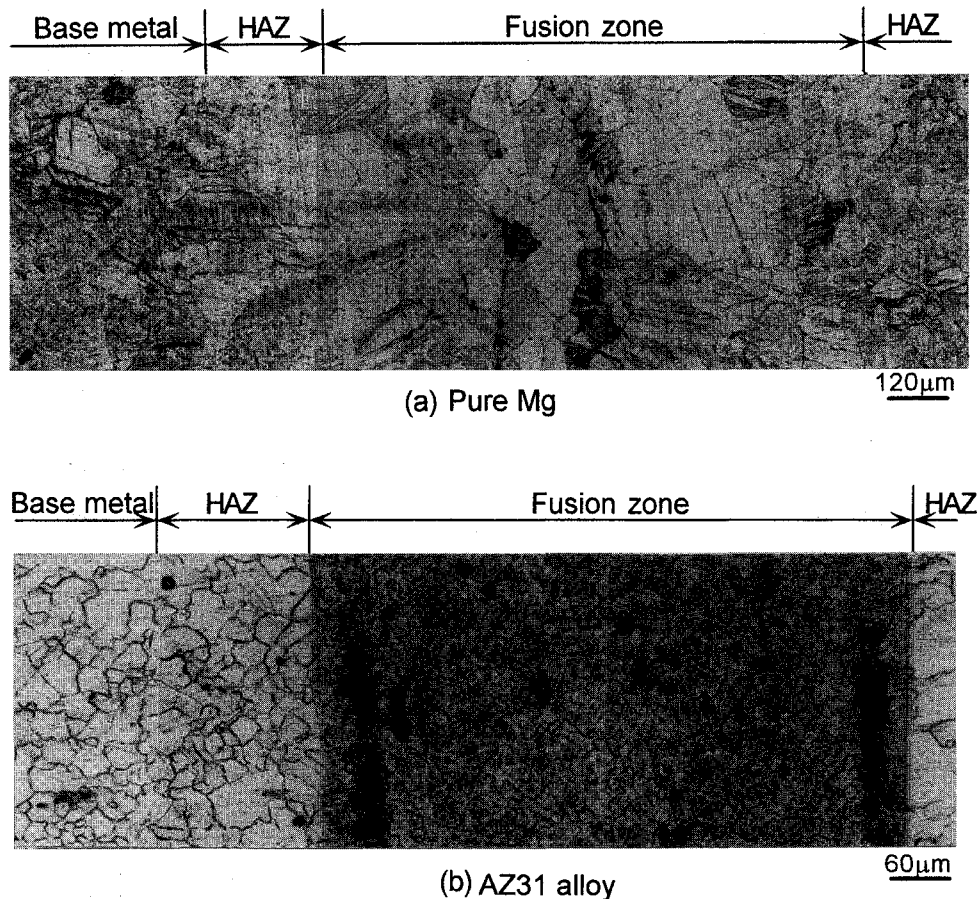


Fig. 3 Microstructures of electron beam welded joints at welding speed 5.83 mm/s .

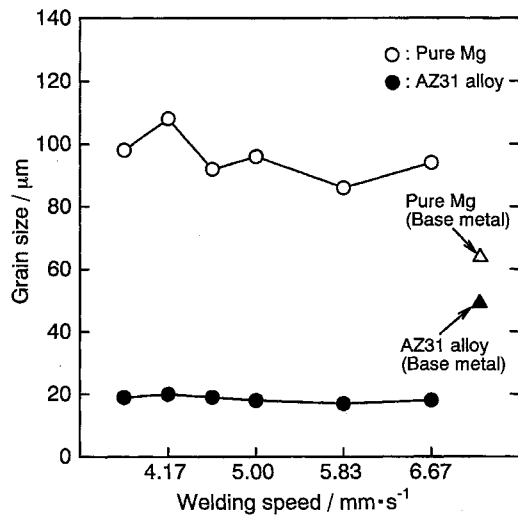


Fig. 4 Relation between welding speed and grain size in fusion zone of electron beam welded joints.

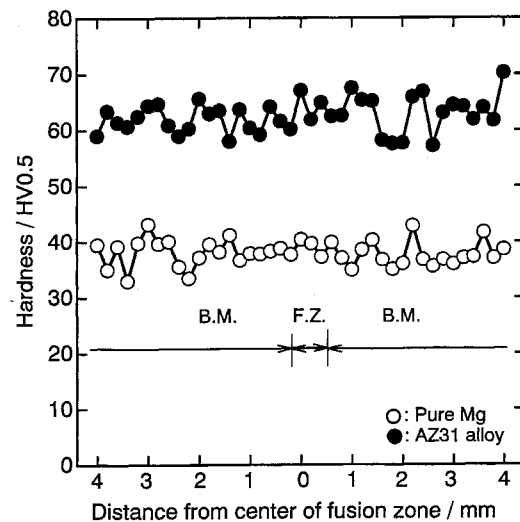


Fig. 5 Hardness distributions of electron beam welded joints at welding speed 5.83 mm/s.

ture, banded grain boundaries were also observed in the heat affected zone and fusion zone. It is presumed that they were caused by grain boundary reaction type precipitation which discontinuously precipitates equilibrium phases from grain boundary. This phenomenon was conspicuous in the heat affected zone. Pearlite-like structure was not observed because the fusion zone had been quenched and there was the dispersion of a chemical compound deemed to be $Mg_{17}Al_{12}$. This was also observed in an EB welded AZ80 joint.²⁾ Welding speed dependency was not observed in the structure of the cross-section and surface of the fusion zone. Coarse columnar crystals and feather structure were not observed in the fusion zone of the EB welded joints of AZ31 alloy and the coarsening of crystal grains in the fusion zone was not seen even in the slow welding speed condition of 3.75 mm/s.

The relation between welding speed and grain size in the cross-section of the fusion zone is shown in Fig. 4. The influence of welding speed on the crystal grain of the cross-section of the fusion zone is not observed in the two base metals. Grain size of the fusion zone of pure Mg is about 90 μm and coarser than that of the base metal, about 64 μm , and the width of columnar crystal in the interface of joint surface is also coarse of about 90 μm .

With AZ31 alloy, the grain size of the fusion zone is about 18 μm or about 36% of that of the base metal about 50 μm . The TIG welded molten metal grain sizes of the pure Mg and AZ31 alloy were 120 μm ⁶⁾ and 68 μm ⁴⁾ respectively, and in EB welded grain sizes of the two materials, are finer than those of TIG welding. This tendency is especially remarkable with the AZ31 alloy. This is because high density welding energy was concentrated into a narrow area as mentioned above, it is thought.

3.2 Hardness distribution of welded joints

As an example of hardness distribution at the center of the joint cross section, the results of the tests with specimens welded at the speed of 5.83 mm/s are shown in Fig. 5. With the pure Mg alloy, although hardness fluctuation is observed in the fusion zone, values are nearly constant and almost the

same as those of the base metal. In the case of AZ31 alloy joints, no difference is observed in hardness in the fusion zone, same as for the pure Mg joints, and values are the same as those of the base metal. This phenomenon is also observed at other welding speeds and no change in hardness is observed, in spite of a great difference in grain size in the fusion zone and base metal. The same phenomenon has also been observed in TIG⁴⁾ and friction welded joints,⁷⁾ and this is a peculiar phenomenon to magnesium alloy welded joints, it is thought.

3.3 Tensile properties

The results of tensile test are shown in Fig. 6. Regardless of the welding speed, the tensile strength of the pure Mg joints is almost the same value as that of the base metal, and joint efficiency which is the ratio between joint tensile strength and base metal tensile strength is 100%. The tensile strength of the AZ31 alloy joints shows a satisfactory value of 99.7% at the welding speed of 5.00 mm/s or faster and, although the highest value was obtained at 5.83 mm/s, the values are a little lower at 4.58 mm/s or slower.

No effect of welding speed on elongation is observed in the pure Mg and the value is about 54% of the elongation of the base metal at all welding speeds. The AZ31 joints indicate slightly higher values at the welding speed of 5.00 mm/s and 5.83 mm/s, but were about 20% of that of the base metal. In the case of TIG welded joints,⁴⁾ joint efficiency was about 80% and elongation was 60% of that of the base metal. Joint efficiency showed favorable values in this test but elongation decreased remarkably. From the authors research on the EB welded joints of AZ61 magnesium alloy, the improvement of elongation was observed when the structure of fusion zone was homogenized by post heat treatment in comparison with joints as welded.⁸⁾ In this test, tests were carried out using joints as welded and the location of fractures was either in fusion zones or at weld interfaces. It is thought, therefore, that the decrease of elongation resulted from the structural unevenness of the fusion zone. And difference in crystal grain sizes between the base metal and the fusion zone, in addition,

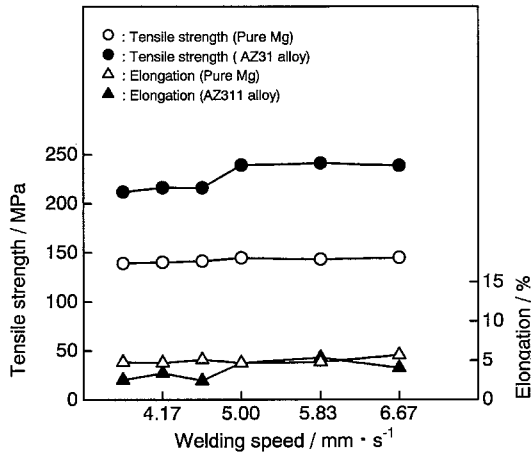


Fig. 6 Relation between welding speed and tensile properties of electron beam welded joints.

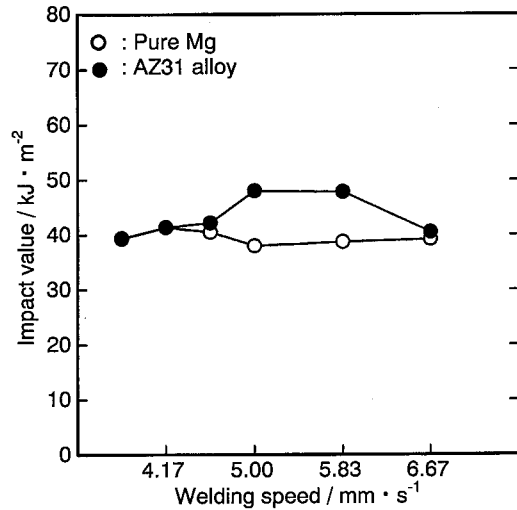


Fig. 8 Relation between welding speed and impact value of electron beam welded joints.

Materials	Welding speed (mm/s)	Fractured position	Fractured surface	Fractograph
Pure Mg	3.75			
	5.83			
AZ31 alloy	3.75			
	5.83			

Fig. 7 Fractured positions and fractographs of tensile tested specimens of electron beam welded joints.

from the exceedingly narrow width of the fusion zones.

Figure 7 shows examples of the location of fractures and fractographs after tensile tests. Pure Mg alloy joints were fractured at the center of the fusion zones, that is, at the points of the convergence of crystal grains which grew from the interface of both sides. In addition, they were ductile fractures where equi-axed dimples and long narrow dimples were observed, but no effect of welding speed on the size of the dimples was observed. In AZ31 joints, cracks started in the interfaces between the fusion zones and base metals and frac-

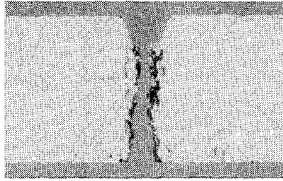

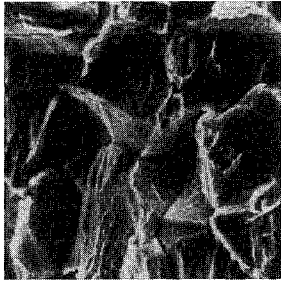
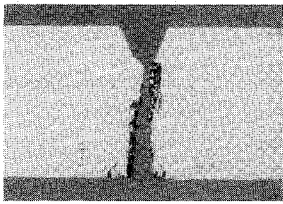

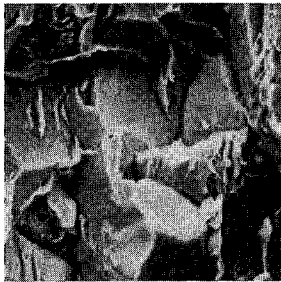
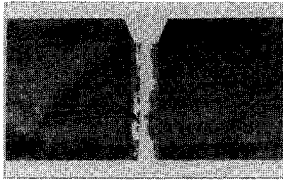

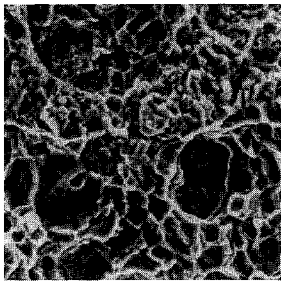
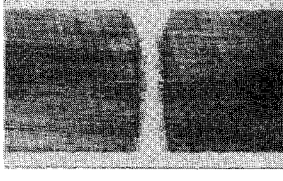

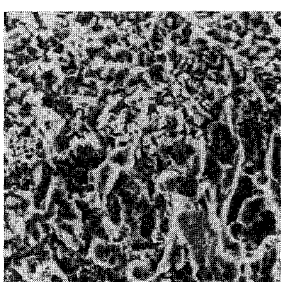
tures were characterized by zigzag lines since these cracks were continuously crossing the fusion zones. On the observation of fractures, the presence of large diameter dimples in the heat affected zones and small diameter dimples in the fusion zones are observed. Partially brittle fractures are also identified in the fusion zones. The dimple diameter slightly decreased at the welding speed of 5.83 mm/s in comparison with 4.17 mm/s.

While TIG welded AZ31 alloy joints⁴⁾ were fractured rectilinearly crossed at the center of the fusion zone, the fractured area of EB welded joints showed a different aspect. This is because, it is thought, the fusion zone width of EB welded joints was considerably narrower than that of TIG welded joints. Also tensile stress concentrated onto the weld interface due to a rapid change in crystal grain sizes of the fusion zones and the base metal. In addition, the structure of the fusion zones is not uniform as mentioned before. Also the fusion zones with fine crystal grains are in the state of the mixture of dimple pattern which is peculiar to ductile fracture and the flat facet of brittle fracture, and this is thought to be one of the reasons for the decrease of joint ductility.

3.4 Impact properties

Figure 8 shows the results of impact test using specimens having a notch at the center of the fusion zone. Welding speed dependency is not observed in the impact values of the pure Mg joints and values are almost the same as that of the base metal. However, the highest impact value of the AZ31 alloy was marked at the welding speed of 5.00 and 5.83 mm/s and it was about 87% of that of the base metal.

Figure 9 shows the location of fracture and fractographs of the impact tested specimens. The pure Mg joints were fractured in the fusion zone and the AZ31 alloy joints also in the fusion zone, the same as tensile test, but there was a lot of unevenness on fractures. This is because, it is thought, fractures started, in the case of pure Mg, in the vicinity of the final solidification area at the center of the fusion zones. In the case of AZ31 alloy, it seems that cracks occurred in the vicinity of interfaces of the base metal and the fusion zone, that is, the

Materials	Welding speed (mm/s)	Fractured position	Fractured surface	Fractograph
Pure Mg	3.75			
	5.83			
AZ31 alloy	3.75			
	5.83			

3mm 3mm 20μm

Fig. 9 Fractured positions and fractographs of impact tested specimens of electron beam welded joints.

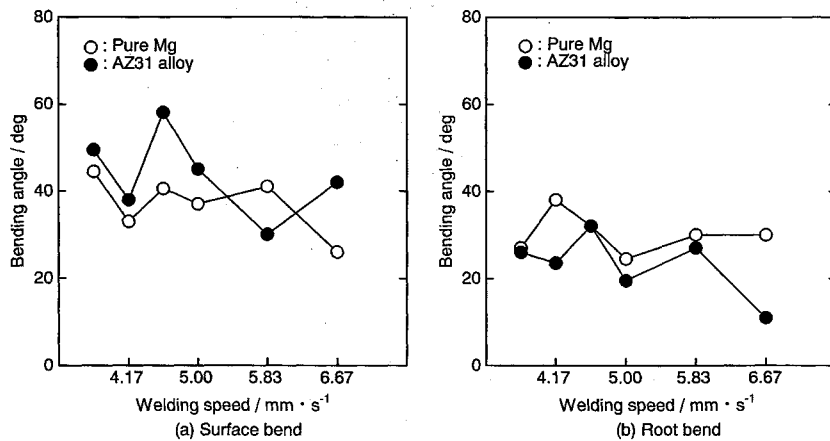


Fig. 10 Relation between welding speed and bending angle of electron beam welded joints.

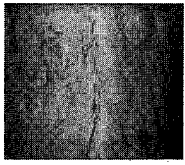
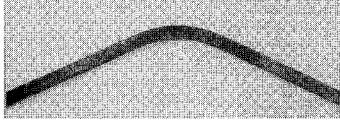
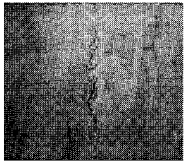
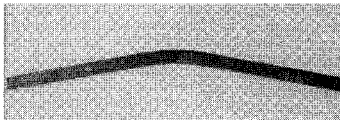
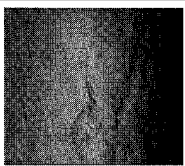

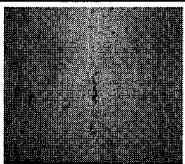

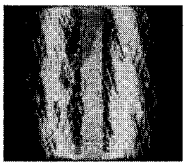

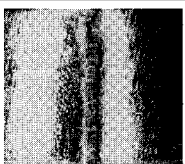




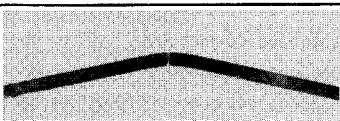
Materials	Welding speed (mm/s)	Bend test	Cracked surface	Bending angle
Pure Mg	3.75	Surface bend		 Bending angle : 50°
		Root bend		 Bending angle : 21°
	5.83	Surface bend		 Bending angle : 40°
		Root bend		 Bending angle : 30°
AZ31 alloy	3.75	Surface bend		 Bending angle : 51°
		Root bend		 Bending angle : 26°
	5.83	Surface bend		 Bending angle : 38°
		Root bend		 Bending angle : 27°

Fig. 11 Surface appearances and bending angle of bending tested specimens of electron beam welded joints.

weld interface, since the width of the fusion zone is narrower, and progressed in zigzags through the fusion zone and then it was fractured.

In the EB welded joints of steel, if Charpy impact test is carried out with specimens having a notch at the center of weld metal, sometimes the route of the crack veers toward the base metal side. It has been reported that the reason for this is closely related to the bead width and hardenability of weld metal.⁹⁻¹¹⁾ However, no systematic change in hardness as seen in magnesium alloys is observed and it is thought that

there is no influence of the hardness of the fusion zone. In the case of magnesium alloys, therefore, it is thought that cracks which occurred in impact test progressed into the weld interface where there were differences in crystal grain diameters. The reason why their bead widths are narrow and the structure of the fusion zone, that is the area where a notch was made on impact test specimens, is extremely fine compared with the base metal. In addition, although a slight cross-sectional contraction was observed on the two test materials, no influence of welding speeds on the aspect of fractures was

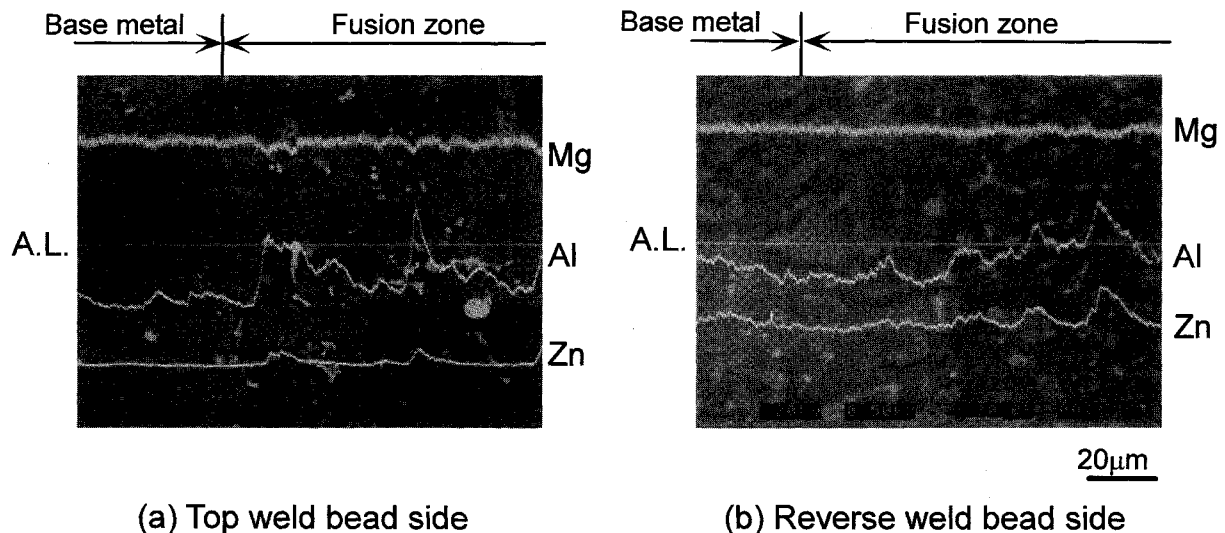


Fig. 12 EDX analysis line profiles of Al, Zn and Mg across the weld bond of electron beam welded AZ31 alloy joint at welding speed 5.00 mm/s.

seen. As a result of fracture observation, it was found out that the unevenness of fractures was less with the pure Mg and coarse dimples and cleavage fractures which were fractured at grain boundaries were observed. There was considerable unevenness in the fractured surfaces of the AZ31 alloy and fine equi-axed dimples were seen verifying that impact values were higher than those of the pure Mg.

3.5 Bending properties

Figure 10 shows the results of bending test. Both pure Mg and AZ31 alloy showed slightly higher face bending angle than root bending angle. As shown in the macrostructure in Fig. 2, heterogeneous welding metal which solidified discontinuously is clearly observed in the vicinity of the penetration beads. This is thought to be the cause of the low bending angle of penetration beads. Both surface and root bead bending angles tend to decrease as welding speed increase and this phenomenon was clearly observed in the AZ31 alloy. The bending angles of the pure Mg were about 45% lower than that of the base metal in every welding condition. Both surface and root bending angles of the AZ31 alloy showed the highest values at the welding speed of 4.58 mm/s but these values were fairly low, about 40% lower than that of the base metal. This is presumed to be the same as the cause of the decrease in elongation in tensile properties.

Figure 11 shows examples of the situation of crack occurrence after the bending test and bending angle. In the pure Mg, cracks generated at the center of the fusion zones and progressed spreading into branches. On the other hand, it was found that the cracks of AZ31 alloy generated in the vicinity of the fusion zones at the end of the test specimens and progressed into the fusion zones in zigzags. This tendency was the same in the case of tensile and impact tests.

3.6 Chemical analysis of welds

Figure 12 shows the results of the EDX analysis of aluminum, zinc, and magnesium near the top and reverse on the cross-sections of the AZ31 alloy joints which were welded at the speed of 5.00 mm/s and they showed excellent tensile and

impact properties. On the top bead side, the tendency of a slight decrease only in zinc from the heat affected zones was observed but no changes were seen in aluminum and magnesium concentrations. On the reverse bead side, no changes in chemical composition due to welding were observed.

In the case of EB welded 5052 aluminum alloy, it has been reported that magnesium, an alloy component, in the weld metal was diluted due to evaporation and this evaporation of alloy component decreased the hardness of the weld metal as well as tensile strength of the welded joint.³⁾ In the case of AZ31 alloy, there was no change in the hardness of the fusion zone and tensile strength was the same as that of the base metal. However, it is considered that the conspicuous decreases in elongation or bending angle in joint tensile and bending tests were somewhat affected by the evaporation of the alloy components.

4. Conclusion

Upon the investigation of the structures and mechanical properties of the EB welded industrial pure Mg and structural AZ31 alloy joints, the following results were obtained.

- (1) Satisfactory bead appearance without any defects was obtained in both the pure Mg and AZ31 alloy joints.
- (2) The crystal grains of the pure Mg molten metal were coarser than those of the base metal, however, they were extremely fine in the AZ31 alloy.
- (3) The tensile strength and impact properties of the pure Mg were almost the same as those of the base metal, regardless of welding speed. In the case of AZ31 alloy, excellent tensile strength and impact properties were obtained at the welding speed of 5.00 and 5.83 mm/s. However, the decrease of elongation was considerable in both the materials.
- (4) Some decrease of zinc was observed in the heat affected zone of the top weld bead side of the AZ31 alloy.

From these results, it became clear that the EB weldability of both the materials was excellent in the range of this experiment. However, for the application and practical use of magnesium alloys, the improvement of brittleness which greatly

decreases in comparison with the base metal is the important problem to be solving in the future.

Acknowledgments

A part of this research is supported by a grant from the Light Metals Educational Foundation. Authors wish to express our sense of gratitude by making special mention here.

REFERENCES

- 1) S. Sugiyama: *J. Light Metal Welding & Construction* **34** (1996) 18–30.
- 2) T. Asahina, M. Ohkubo and H. Tokisue: *J. Japan Inst. Light Metals* **44** (1994) 210–215.
- 3) H. Nagai: *J. Light Metal Welding & Construction* **21** (1983) 355–365.
- 4) T. Asahina and H. Tokisue: *J. Japan Inst. Light Metals* **45** (1995) 70–75.
- 5) T. Asahina, K. Katoh and H. Tokisue: *J. Japan Inst. Light Metals* **45** (1995) 453–458.
- 6) T. Asahina and H. Tokisue: *Proceedings of the 87th Annual Meeting of Japan Inst. Light Metals* **87** (1994) 259–260.
- 7) T. Asahina, K. Katoh and H. Tokisue: *J. Japan Inst. Light Metals* **41** (1991) 674–680.
- 8) T. Asahina and H. Tokisue: *Proceedings of the 98th Annual Meeting of Japan Inst. Light Metals* **98** (2000) 271–272.
- 9) Y. Arata, F. Matsuda, Y. Shibata, S. Hozumi, Y. Ono and S. Fujihira: *Quarterly J. Japan Welding Society* **44** (1975) 1011–1017.
- 10) Y. Arata, F. Matsuda, Y. Shibata, Y. Ono, M. Tamaoki and S. Fujihira: *Quarterly J. Japan Welding Society* **48** (1979) 598–605.
- 11) K. Satoh, M. Toyoda, K. Nohara, S. Takeda and M. Nayama: *Quarterly J. Japan Welding Society* **51** (1982) 679–686.